Engineering with Computers (2024) 40:1559–1573
https://doi.org/10.1007/s00366-023-01884-x

ORIGINAL ARTICLE

Application of the Bezier integration technique with enhanced stability in forward dynamics of constrained multibody systems with Baumgarte stabilization method

Mohammad Khoshnazar[1] · Mohammad Dastranj[1] · Ali Azimi[1] · Mohammad M. Aghdam[1] · Paulo Flores[2]

Received: 8 February 2023 / Accepted: 3 August 2023 / Published online: 12 August 2023

Abstract
This paper deals with the study and application of a numerical integration scheme based on the Bézier curves to obtain stable and accurate solutions of the governing differential–algebraic equations (DAEs) of constrained multibody systems. For this purpose, the standard Lagrange multiplier method is utilized to derive the equations of motion for constrained mechanical systems. It is well known that constraints violation and instability are amongst the main computational difficulties of various numerical integration algorithms to provide accurate solutions for DAEs. In the present study, the Baumgarte stabilization technique is employed, as well as a criterion to select the Baumgarte parameters based on the stability domain analysis. Stability regions based on dimensionless Baumgarte parameters are obtained for different orders of Bézier curves together with other classic numerical integration algorithms, namely the Adams–Bashforth and Runge–Kutta techniques. It is shown that the proper identification and selection of Baumgarte parameters is highly dependent on the integration scheme utilized. A comparative analysis performed within the present work reveals that the Bézier method provides substantially wider region of stability for the same level of computational effort. A planar slider-crank mechanism is considered as an example of application to demonstrate and implement the Bézier technique, which permits to examine the benefits of the presented stability analysis. It is demonstrated that for certain values of Baumgarte parameters, the Bézier method remains stable, while other methods become unstable. Due to the good performance of the applied method based on the Bézier approach, both in terms of efficiency and stability, it is expected that the introduced integration method to be used for various benchmark studies performed under the umbrella of multibody dynamics.

Keywords Bézier curves · Baumgarte stabilization method · DAEs · Stability regions · Constraint violation

1 Introduction

In the process of modeling and simulating the dynamics of constrained multibody systems, it is common to use formulations based on non-minimal coordinates, due to their flexibility in developing general computer codes. In this approach, Newton–Euler's laws of motion are usually utilized for each rigid body within the mechanical system under analysis, leading to Ordinary Differential Equations (ODEs), while algebraic equations are added in order to reflect the kinematic constraints, which are typically associated with mechanical joints. This process results allows to obtain the equations of motion in the form of a set of Differential Algebraic Equations (DAEs) [1, 2]. It has been recognized that there are alternative formulations to derive the equations of motion for constrained multibody systems, such as the ones purposed by Lagrange [3], Hamilton [4], Gibbs [5], Dirac [6], Kane [7, 8] and Udwadia-Kalaba [9]. These methodologies differ in the type of coordinates considered and methods utilized to handle the violation of constraints, which results in different aspects such as computational errors [10, 11]. The problem of formulating and solving the violation of constraints in multibody systems has been the subject of intense investigation over the last decades. The interested

✉ Ali Azimi
aliazimi@aut.ac.ir

[1] Department of Mechanical Engineering, Amirkabir University of Technology (Tehran Polytechnic), Hafez Ave, Tehran 15914, Iran

[2] CMEMS-UMinho, Departamento de Engenharia Mecânica, Universidade Do Minho, Campus de Azurém, 4804-533 Guimarães, Portugal

reader in further details is referred to the following references [12–20].

A common approach to numerically solve the equations of motion of constrained multibody systems developed in the form of DAEs relies on time-differentiation of the constraint equations, resulting in a system of ODEs. In most of practical cases, analytical solutions are not available and therefore, numerical integration methods have been employed [21]. A wide variety of numerical approaches have been proposed over the last decades, namely those based on one-step schemes, such as the Euler algorithm, multi-stage single-step schemes, such as the Runge–Kutta method, and multi-step techniques, such as the Adams–Bashforth method. All of these methods are applied to first order ODEs and therefore, it is necessary to convert a generally nth order ODE to a system of n first order ODEs, using appropriate techniques of changing variables. With the standard Lagrange multiplier technique, the kinematic constraint is incorporated only at the acceleration level [22]. Hence, violation of constraints occurs at position and velocity levels due to numerical errors associated with the integration process. Amongst the several different approaches introduced to eliminate or, at least, minimize those numerical errors [23–25], one may refer to the Baumgarte stabilization method [23], in which appropriate terms related to the problem of constraints violation at the position and velocity levels are added to the ODE system. The main difficulty associated with the Baumgarte stabilization method deals with the identification of the parameters for the feedback values of constraints and their first-time derivatives. The selection of appropriate Baumgarte parameters to obtain the accurate solution in terms of violation of constraints is still a challenging issue within the field of multibody dynamics [22].

Chang and Nikravesh [26] developed an adaptive method to determine the proper Baumgarte parameters and demonstrated the effectiveness of the proposed method using two benchmark examples. Yoon et al. [27] used pseudo-integration of the constraint dynamics to investigate the stability of the Baumgarte method, and to identify and select the appropriate values for the Baumgarte coefficients. Ostermeyer [28], dealt with control aspects to explain the effects of the Baumgarte method together with presenting some rules to choose the values of the corresponding parameters. The works by Lin and co-workers [29, 30] showed that there exists a criterion for the proper selection of the Baumgarte parameters that results in a stable and accurate solution. The criterion proposed is dependent on the numerical integration method considered to solve the equations of motion. Flores et al. [31] presented a parametric study on the Baumgarte method to study the influence of the values of Baumgarte parameters, integration method, time step size, and accuracy of the initial conditions. In turn, Kim et al. [32], Ascher et al. [33, 34] and Guizhi and Rong [35] developed different techniques to select Baumgarte parameters. Park and co-workers [36, 37] proposed a constraint stabilization approach similar to the Baumgarte method considering a penalty formulation of the constraint equations. Bayo and Avello [38] presented an augmented Lagrangian formulation based on the Hamilton canonical form of the equations of motion, which ensures better accuracy and robustness in the presence of singular configurations compared with the alternative approach derived by Bayo et al. [25]. Weijia et al. [39] proposed an automatic constraint violation stabilization method for the numerical integration of equations of motion in the dynamics of multibody systems. Blajer [40] developed a powerful methodology for the exact elimination of the constraint violations, which is based on appropriate corrections of the state variables after each integration step. Hong and co-workers [41] presented an implicit constraint enforcement technique that is stable for large time steps and does not require problem-dependent stabilization parameters. In a later work, these authors described their method for rigid body simulations with both holonomic and non-holonomic constraints [42]. Braun and Goldfarb [43], by means of the Udwadia–Kalaba approach, proposed an explicit equation of constrained motion by embedding a small virtual force and a small virtual impulse in the equation of motion. Nada and Bayoumi [44] developed a constraint stabilization method for multibody systems based on fuzzy logic control for both holonomic and non-holonomic constraints. The interested reader in a detailed and comprehensive analysis of different methodologies for the constraint enforcement under the framework of multibody systems is referred to the works by Laulusa and Bauchau [45, 46].

Using Bézier curves, Aghdam et al. [47] presented a multi-step method to solve the initial value problems. These authors showed that the stability of the Bézier based solution is enhanced when comparing with other well-known methods, namely the well-established Adams–Moulton approach. Furthermore, consistency and convergence of the method are investigated using error analysis theorems for multi-step approaches [47]. Subsequently, a combination of the Bézier method and the differential quadrature technique was utilized to solve the governing Partial Differential Equations (PDEs) arising in the transient response of composite plates [48] and conical shells [49]. More recently, the Bézier multi-step method was considered to obtain numerical solutions for nonlinear vibration and post-buckling of nanocomposite beams [50] and stress analysis of notched nanocomposite plates [51]. It is noteworthy that Bézier curves are based on the Bernstein basis polynomials and some given points, called control points. These curves are widely utilized in computer graphics and computer-aided design, due to their

smooth nature. More details on Bézier curves and their properties can be found in references [52, 53].

Thus, in the present study, the Bézier integration technique is utilized to obtain numerical solutions for the DAEs of constrained multibody mechanical systems, by introducing a numerical integration scheme for the resulted system of ODEs. The stability domains of dimensionless Baumgarte parameters are established for different orders of the Bézier method. The stability regions are examined and compared with those of some classical integration methods, such as the Adams–Bashforth and Runge–Kutta algorithms, which permit to show the benefits and gains associated with the Bézier integration technique. Finally, a planar slider-crank mechanism is considered as a benchmark example for applications, which serves to highlight the benefits of the proposed methodology. It is noted that a planar slider-crank mechanism was used in [54] as a benchmark mechanism. A variation of the slider-crank mechanism is also introduced in [55] for evaluating various formulations and integration techniques used in simulation and analysis of multibody systems with kinematic constraints.

2 Equations of motion for constrained multibody systems

This section addresses the main aspects related to the formulation of the equations of motion of constrained multibody mechanical systems. Thus, for a general multibody mechanical system, the kinematic constraints can be established as a set of linear and/or nonlinear holonomic algebraic equations as [1]

$$\mathbf{c}(\mathbf{q}, t) = 0 \tag{1}$$

where $\mathbf{c}(\mathbf{q}, t) = [\mathrm{c}_1(\mathbf{q}, t), \ldots, \mathrm{c}_m(\mathbf{q}, t)]^{\mathrm{T}}$ represents the m-vector of constraint equations, $\mathbf{q} = [q_1, \ldots, q_n]^{\mathrm{T}}$ denotes the n-vector of generalized coordinates, and t is the time variable.

The dynamic equations for constrained multibody systems can be expressed by [1]

$$\mathbf{M}\ddot{\mathbf{q}} + \mathbf{C}_{\mathbf{q}}^{\mathrm{T}}\boldsymbol{\lambda} = \mathbf{g} \tag{2}$$

where $\mathbf{M}$ represents the generalized mass matrix,$\ddot{\mathbf{q}}$ denotes the vector of generalized accelerations,$\mathbf{C}_{\mathbf{q}}$ is the Jacobian matrix of the constraint equations,$\boldsymbol{\lambda}$ represents the vector of Lagrange multipliers, and $\mathbf{g} = \mathbf{g}(t, \mathbf{q}, \dot{\mathbf{q}})$ contains the applied generalized forces that may include the Coriolis and centrifugal forces. The unknowns in Eq. (2) are the vector of accelerations $\ddot{\mathbf{q}}$ and the vector of Lagrange multipliers $\boldsymbol{\lambda}$, resulting in a total of $n+m$ unknowns. Since Eq. (2) contains only n equations, in order to be able to solve them, it is required to consider the additional m kinematic constraint equations. Thus, differentiating Eq. (1) with respect to time yields the velocity constraint equations as

$$\mathbf{C}_{\mathbf{q}}\dot{\mathbf{q}} = -\mathbf{c}_t \tag{3}$$

where $\dot{\mathbf{q}}$ represents the vector of generalized velocities, and the subscript t indicates partial differentiation with respect to time. A second differentiation of Eq. (1) with respect to time leads to the acceleration constraint equations in the form of

$$\mathbf{C}_{\mathbf{q}}\ddot{\mathbf{q}} = -\left(\mathbf{C}_{\mathbf{q}}\dot{\mathbf{q}}\right)_{\mathbf{q}}\dot{\mathbf{q}} - 2\mathbf{C}_{\mathbf{q}t}\dot{\mathbf{q}} - \mathbf{c}_{tt} \equiv \boldsymbol{\gamma} \tag{4}$$

in which $\boldsymbol{\gamma}$ represents the right-hand side of acceleration equations. Equations (1), (3), and (4) must be satisfied during the numerical solution of the equations of motion for constrained multibody mechanical systems. Therefore, Eqs. (2) and (4) can be condensed in the matrix form as

$$\begin{bmatrix} \mathbf{M} & \mathbf{C}_{\mathbf{q}}^{\mathrm{T}} \\ \mathbf{C}_{\mathbf{q}} & 0 \end{bmatrix} \begin{bmatrix} \ddot{\mathbf{q}} \\ \lambda \end{bmatrix} = \begin{bmatrix} g \\ \gamma \end{bmatrix} \tag{5}$$

It is clear that Eq. (5) contains $n+m$ equations and $n+m$ unknowns. Assuming that the mass matrix is positive definite and the Jacobian matrix has a full row rank, a unique solution for accelerations $\ddot{\mathbf{q}}$ and Lagrange multipliers $\boldsymbol{\lambda}$ will be obtained. It is noted that necessary and sufficient conditions for the existence and uniqueness of solutions for accelerations and Lagrange multipliers are obtained and discussed in [56]. Then, in each integration time step, velocities and positions, for the next time step, can be computed by integrating the accelerations and velocities of the previous step. This procedure is repeated until the final analysis time is reached in forward dynamic problems [1, 31].

3 Baumgarte stabilization method

The main purpose of this section is to summarize the key issues associated with the Baumgarte stabilization method and its incorporation into the equations of motion for constrained multibody systems. Thus, when using Eq. (5) in its original form, it is guaranteed that the constraint equations at the acceleration level, $\ddot{\mathbf{c}} = 0$, are satisfied at every integration step. Furthermore, as it was mentioned previously, $\dot{\mathbf{c}} = 0$, and $\mathbf{c} = 0$ must also be satisfied in any numerical integration method that is used to solve the equations of motion of the system. However, from the control theory it is known that the equation $\ddot{\mathbf{c}} = 0$ represents an unstable system, therefore $\mathbf{c}$ and $\dot{\mathbf{c}}$ will not converge to zero if any perturbation occurs during numerical integration [29, 57].

Thus, based on the Baumgarte constraints stabilization technique, the acceleration constraint equation is modified and rewritten as [23]

$$\ddot{\mathbf{c}} + 2\alpha\dot{\mathbf{c}} + \beta^2\mathbf{c} = 0 \tag{6}$$

where α and β are two scalar positive coefficients. By taking the Laplace transform of Eq. (6), the characteristic equation would be [58]

$$s^2 + 2\alpha s + \beta^2 = 0 \tag{7}$$

From the control theory, it is established that with α and β greater than zero, Eq. (7) is stable and, consequently, $\mathbf{c}$ and $\dot{\mathbf{c}}$ will converge to zero. Hence, Eq. (4) can be rewritten as

$$\mathbf{C_q}\ddot{\mathbf{q}} = \boldsymbol{\gamma} - 2\alpha\dot{\mathbf{c}} - \beta^2\mathbf{c} \tag{8}$$

Finally, the equations of motion can be expressed as

$$\begin{bmatrix} \mathbf{M} & \mathbf{C}_\mathbf{q}^{\mathrm{T}} \\ \mathbf{C_q} & 0 \end{bmatrix} \begin{bmatrix} \ddot{\mathbf{q}} \\ \lambda \end{bmatrix} = \begin{bmatrix} g \\ \gamma - 2\alpha\left(\mathbf{C_q}\dot{\mathbf{q}} + \mathbf{c}_t\right) - \beta^2 c \end{bmatrix} \tag{9}$$

While the Baumgarte constraints stabilization method gives accurate results in some cases, there is no valid method for selecting the parameters α and β [22, 26, 31, 33]. As it was pointed out by Baumgarte, the suitable parameters are obtained by numerical experiments [23]. It should be noted that improper selection of the Baumgarte coefficients can lead to unacceptable results in terms of the physics associated with the dynamic response of the constrained multibody mechanical systems.

4 Selection of α and β parameters for the Bézier method

In this section, a general study on the identification and selection of the Baumgarte parameters in the context of the Bézier integration technique is presented. It has been recognized that positive values for α and β parameters does not guarantee the convergence of $\mathbf{c}$ and $\dot{\mathbf{c}}$ [29, 30]. This aspect suggests that the selection of the values for α and β only based on the stability of Eq. (6) does not guarantee appropriate results when simulating constrained multibody systems.

At this stage, it must be highlighted that the numerical integration algorithms convert differential equations to discretized equations and then solve them. Different numerical integration algorithms are available for the discretization process. Therefore, it is important to check the stability conditions of the discretized resulting equations rather than the original differential equations [29]. This aspect is of crucial relevance, since the selection of adequate values for the α and β parameters also depends on the integration method being utilized in the process of solving the equations of motion.

Using Bézier curves, a new multi-step method for the solution of ordinary differential equations was derived by Aghdam et al. [47]. Different degrees of Bézier curves lead to distinctive formulations, as it is listed in Table 1. In what follows, the 2nd order Bézier method is utilized to illustrate how to select Baumgarte parameters based on the stability analysis. The procedure described here, which has been implemented on other numerical integration algorithms [29–31, 35], is based on the stability analysis approach in digital control theory.

The differential equation to be solved by numerical integration can be defined as

$$\dot{y} = f(y, t) \tag{10}$$

where y represents the dependent variable in the differential equation, and $\dot{y}$ is its time derivative.

Applying the Laplace transform technique to Eq. (10) yields

$$sY(s) = F(s) \text{ or } \frac{F(s)}{Y(s)} = s \tag{11}$$

in which s denotes the variable of the Laplace domain.

Thus, when 2nd order Bézier method is considered, the numerical solution of the differential equation can be written as [47]

$$y_{k+1} = y_k + \frac{h}{2}(3f_k - f_{k-1}) \tag{12}$$

where subscript k represents the numerical solution at the corresponding time step, and h denotes the integration time step.

Since Eq. (12) is a discretized equation, the Z transform technique can be utilized for the purpose of studying the stability of the solution [57]. Thus, the Z transform of Eq. (12) can be expressed as

Table 1 The mapping between s and Z planes for the Bézier method

Order	Bézier method formula	Mapping between s and Z plane
2	$y_{k+1} = y_k + \frac{h}{2}(3f_k - f_{k-1})$	$s = \frac{2}{\mathrm{h}}\frac{z(z-1)}{3z-1}$
3	$y_{k+1} = y_k + \frac{h}{12}(19f_k - 8f_{k-1} + f_{k-2})$	$s = \frac{12}{\mathrm{h}}\frac{z^2(z-1)}{19z^2-8z+1}$
4	$y_{k+1} = y_k + \frac{h}{108}(175f_k - 81f_{k-1} + 15f_{k-2} - f_{k-3})$	$s = \frac{108}{h}\frac{z^3(z-1)}{175z^3-81z^2+15z-1}$

$$zY(z) = Y(z) + \frac{h}{2}(3F(z) - \frac{1}{z}F(z)) \tag{13a}$$

or, alternatively,

$$\frac{F(z)}{Y(z)} = \frac{2}{h}\frac{z(z-1)}{3z-1} \tag{13b}$$

where z denotes the Z transform variable.

A direct comparison between Eqs. (11) and (13b) allows to obtain the mapping between s and Z planes as

$$s = \frac{2}{h}\frac{z(z-1)}{3z-1} \tag{14}$$

A similar procedure can be considered to obtain the mapping between s and Z planes for different orders of the Bézier method, results of which are condensed in Table 1.

Introducing Eq. (14) into Eq. (7) the characteristic equation in the Z plane can be obtained and expressed as

$$4z^4 + (-8 + 12\alpha h)z^3 + \left(4 - 16\alpha h + 9\beta^2 h^2\right)z^2 + \tag{15}$$

$$\left(4\alpha h - 6\beta^2 h^2\right)z + \beta^2 h^2 = 0$$

Based on this approach, it can be observed that variable z depends on the values of α, β and h. In order to avoid the dependence on step size, two dimensionless parameters must be established as [29]

$$\widehat{\alpha} = 2\alpha h \text{ and } \widehat{\beta} = \beta^2 h^2 \tag{16}$$

Thus, using these dimensionless parameters, Eq. (15) can be rewritten as.

$$4z^4 + \left(-8 + 6\widehat{\alpha}\right)z^3 + \left(4 - 8\widehat{\alpha} + 9\widehat{\beta}\right)z^2 + (2\widehat{\alpha} - 6\widehat{\beta})z + \widehat{\beta} = 0 \tag{17}$$

Table 2 shows the characteristic equations for different orders of the Bézier method in terms of dimensionless Baumgarte parameters $\widehat{\alpha}$ and $\widehat{\beta}$.

In order to select appropriate values for $\widehat{\alpha}$ and $\widehat{\beta}$ parameters, the behavior of the characteristic equation for different locations of the eigenvalues in the Z plane must be examined first. From control theory, it is known that the stability boundary is the unit circle $|z| = 1$, meaning that $\mathbf{c}$ and $\dot{\mathbf{c}}$ diverge if $|z_p| > 1$ (z_p is z of the pole of the characteristic equation), and converge to zero if $|z_p| < 1$ for all of the poles [59]. Moreover, the smaller the magnitude of $|z_p|$, the faster $\mathbf{c}$ and $\dot{\mathbf{c}}$ converge to zero, and the smaller the magnitude of $\angle z_p$ (angle of z_p), the smaller the frequency of oscillations of $\mathbf{c}$ and $\dot{\mathbf{c}}$. Therefore, in the stability region of the system on the Z plane ($|z| < 1$), according to Eq. (17), a domain for the values of $\widehat{\alpha}$ and $\widehat{\beta}$ can be determined. By specifying the step size, with the use of Eq. (16), the stability region in terms of α and β parameters can then be obtained.

5 Results and discussion

In this section, stability regions for different orders of the Bézier method are presented and discussed, which are based on the approaches described in the previous sections. In order to examine the stability of the Bézier approach, the same stability regions for Adams–Bashforth and Runge–Kutta methods are also studied. Furthermore, a planar slider-crank mechanism is considered as an example of application as a constrained multibody system to study the influence of the values of the Baumgarte parameters on the violation of constraints at the position and velocity levels using different approaches.

5.1 Analysis of the stability regions

The stability regions in terms of $\widehat{\alpha}$ and $\widehat{\beta}$ for the second to the fourth order of the Bézier method are illustrated in the plots of Fig. 1a–c, respectively. In these diagrams, region S is the stable region, $|z_p| < 1$, while region H shows a relatively higher stable domain for the same systems. The

Table 2 Characteristic equations when using different orders of the Bézier method

Order	Characteristic equation
2	$4z^4 + (-8 + 6\widehat{\alpha})z^3 + \left(4 - 8\widehat{\alpha} + 9\widehat{\beta}\right)z^2 + (2\widehat{\alpha} - 6\widehat{\beta})z + \widehat{\beta}$
3	$144z^6 + \left(-288 + 228\widehat{\alpha}\right)z^5 + \left(144 - 324\widehat{\alpha} + 361\widehat{\beta}\right)z^4 + \left(108\widehat{\alpha} - 304\widehat{\beta}\right)z^3 + \left(-12\widehat{\alpha} + 102\widehat{\beta}\right)z^2 - 16\widehat{\beta}z + \widehat{\beta}$
4	$11664z^8 + (-23328 + 18900\widehat{\alpha})z^7 + \left(11664 - 27648\widehat{\alpha} + 30625\widehat{\beta}\right)z^6 + \left(10368\widehat{\alpha} - 28350\widehat{\beta}\right)z^5 + \left(-1728\widehat{\alpha} + 11811\widehat{\beta}\right)z^4 + \left(108\widehat{\alpha} - 2780\widehat{\beta}\right)z^3 + 387\widehat{\beta}z^2 - 30\widehat{\beta}z + \widehat{\beta}$

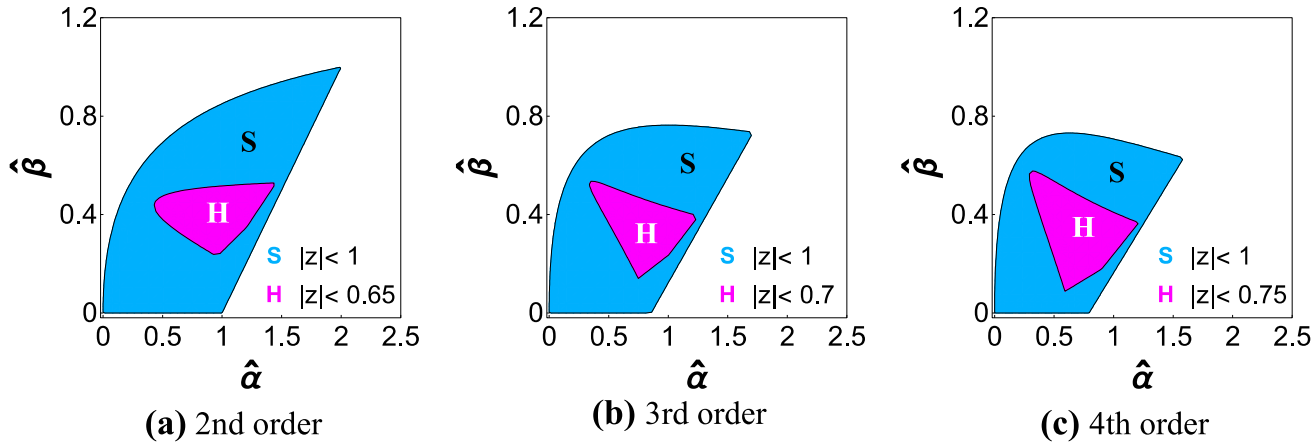

Fig. 1 Stability regions in the $\widehat{\alpha} - \widehat{\beta}$ plane for different orders of the Bézier method

magnitudes of $|z_p|$ for regions H are smaller than 0.65, 0.70, and 0.75 for the second, third, and fourth order of the Bézier method, respectively. As discussed earlier, by choosing $\widehat{\alpha}$ and $\widehat{\beta}$ in these regions, the error of constraint and its derivative converge to zero more rapidly.

It must be noted that the smallest $|z_p|$ that can be found are 0.58, 0.62, and 0.65, respectively for the second, third, and fourth order of the Bézier method. It is noteworthy that for a characteristic equation with orders higher than two, only the dominant eigenvalue, which has the largest $|z_p|$, is considered since it has the greatest effect on the constraint error. Figure 1a–c allow to conclude that the stability regions of the Bézier method slightly decrease as the order of the method increases.

In what follows, a comparison between the stability regions of the Bézier and Adams–Bashforth methods is presented. It should be noted that formulations for the second order of both methods are the same and, therefore, they exhibit similar stability regions. Thus, a comparison is considered between the 3rd and 4th order of Bézier and Adams–Bashforth algorithms, as it is illustrated in the plots of Fig. 2. As it can be observed in the diagram, the Bézier stability regions for both the 3rd and 4th orders are larger than those of the Adams–Bashforth. This fact means that the selection range of Baumgarte parameters for the Bézier method is significantly larger, which can be considered as a clear benefit of the presented method when compared with the Adams–Bashforth method. Moreover, it can be seen that the percentage of reducing the size of stability regions from 3rd order to 4th order of Adams–Bashforth is considerably higher than that of the presented Bézier technique.

The subsequent important study is to examine stability regions for the three different techniques, namely the Bézier, Adams–Bashforth and Runge–Kutta methods. It should be noted that the computational costs of the 4th order Bézier and Adams–Bashforth are quite similar when solving the equations of motion. However, the computational cost of the Runge–Kutta method for the same order is about 5 times higher than Bézier and Adams–Bashforth. It is well-known

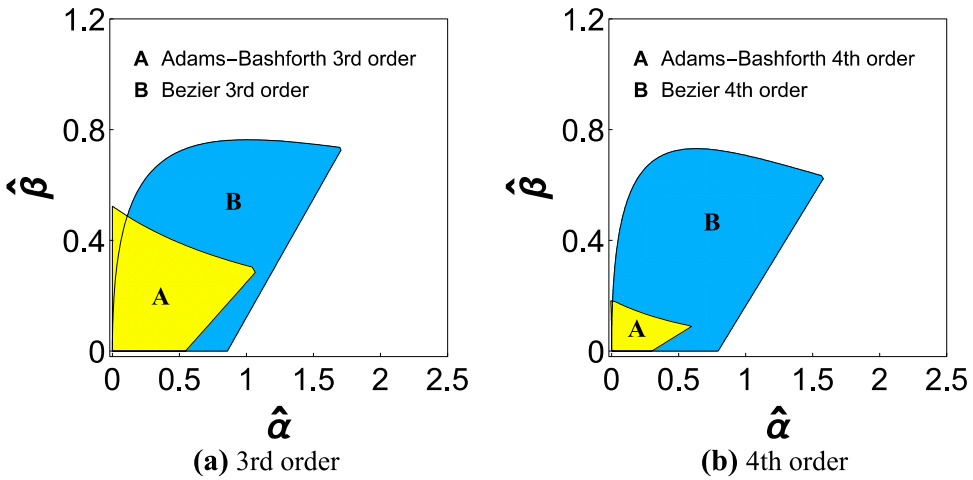

Fig. 2 Comparison between stability regions of Bézier and Adams–Bashforth methods

that computational effort plays a key and decisive role in the identification and selection of the most appropriate numerical procedure to solve the equations of motion. In order to provide a simple and fair comparison, the step size of the Runge–Kutta method should be 5 times greater than the step size for the other two methods, to have a similar computational cost for all three approaches. For comparison, the step size is assumed to be 1 ms for Bézier and Adams–Bashforth methods, and 5 ms for Runge–Kutta. Figure 3 shows the stability regions of the mentioned methods in terms of 2α and β^2. It can be observed that considering similar computational costs, the Bézier method provides the largest stability region, when compared to the other two methods, while Adams–Bashforth exhibits the smallest region.

5.2 Demonstrative example of application

Figure 4 shows a generic configuration of the planar slider-crank mechanism considered in the scope of this study. The geometrical and inertial properties of the mechanism bodies are presented in Table 3. It should be noted that all joints are considered to be ideal, the gravitational effects are present, and the crank is given an initial angular velocity of 10 rpm counter clockwise. The initial conditions at the position and velocity levels are consistent with the physics of the problem, in order to prevent violation of constraints at the initial instant of analysis, which, eventually, can lead to erroneous results [60].

The equations of motion for the slider-crank mechanism can be formulated using an optional set of coordinates. In the formulation considered in the present work, the generalized coordinates are expressed as [29]

$$\mathbf{q} = \begin{bmatrix} \theta_1 & x_2 & y_2 & \theta_2 & x_3 \end{bmatrix}^{\mathrm{T}} \tag{18}$$

where θ_1 and θ_2 represent the angles of bodies 1 and 2 with respect to the horizon, x_2 and x_3 are the horizontal positions of the centers of mass of bodies 2 and 3 (which are considered to be located at the corresponding mid-points), and y_2 denotes the vertical position of the center of mass of body 2.

The equations of the kinematic constraints of the slider-crank multibody model can be established as

$$\mathbf{c} = \begin{bmatrix} l_1\cos(\theta_1) + \frac{l_2}{2}\cos(\theta_2) - x_2 \\ l_1\sin(\theta_1) + \frac{l_2}{2}\sin(\theta_2) - y_2 \\ x_2 + \frac{l_2}{2}\cos(\theta_2) - x_3 \\ y_2 + \frac{l_2}{2}\sin(\theta_2) \end{bmatrix} \tag{19}$$

in which l_1 and l_2 denote the lengths of bodies 1 and 2, respectively. With the set of coordinates represented in Eq. (18) and constraint relations expressed in Eq. (19), the resulted mass matrix, constraint Jacobian matrix, vector $\boldsymbol{\gamma}$ and vector $\mathbf{g}$ are reported in the Appendix presented at the end of the article. Therefore, the equations of motion can be developed as in Eq. (5).

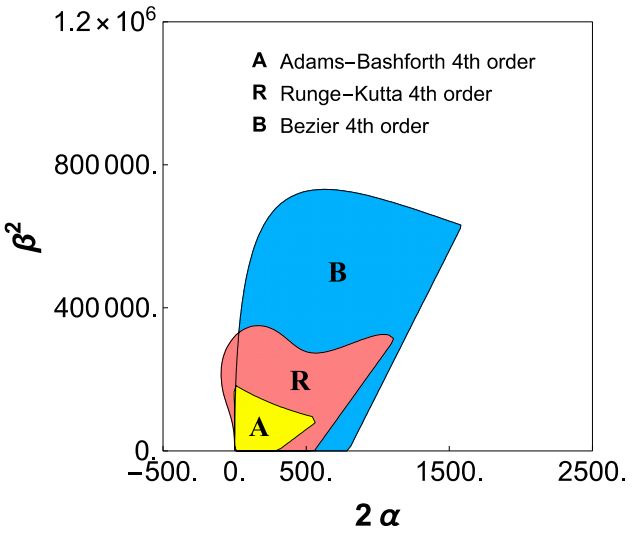

Fig. 3 Comparison between stability regions of Bezier, Adams–Bashforth and Runge–Kutta methods of order 4 with the same computational cost

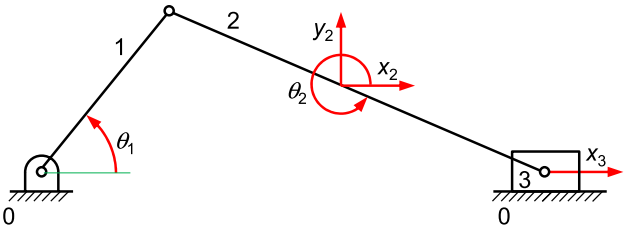

Fig. 4 Planar slider-crank mechanism

5.2.1 Analysis without constraints stabilization

The first analysis performed in this study was to solve the equations of motion of the mechanism using the 4th order of both Bézier and Adams–Bashforth methods with different

Table 3 Properties of the bodies of the slider-crank mechanism [19]

Body number	Length (m)	Mass (kg)	Moment of inertia (kgm^2)
1	0.2	20	45
2	0.35	3.5	3.5
3	–	2.5	0.02

step sizes and without incorporating the Baumgarte stabilization method. Thus, in order to examine the stability of the system, the error of the first constraint in Eq. (19), which represents the x-direction constraint due to the revolute joint between the crank and the connecting rod, is computed. This constraint can be considered as representative of all of the constraints in Eq. (19).

Figure 5 compares the error for the first constraint for both Bézier and Adams–Bashforth techniques. Thus, by analyzing these plots, it can be observed that the constraint violation increases linearly with time. Therefore, after some time, either the amount of error reaches a point that causes serious problems for the system simulation or collapses where the error suddenly increases too much. As it is shown in the plots, for all step sizes considered, the collapse point for the Bézier method occurs later than the Adams–Bashforth method, which is a benefit and gain associated with the Bézier integration technique. The errors in the first constraint for both techniques are compared in Fig. 6 for several step sizes. Figures 5 and 6 indicate that both methods have the same order of error by considering the same step sizes. Furthermore, it can be observed that the constraint error for 4th order Bézier is slightly less than 4th order Adams–Bashforth in different step sizes. In particular, the Bézier method provides more stable and even more accurate results for large step sizes,

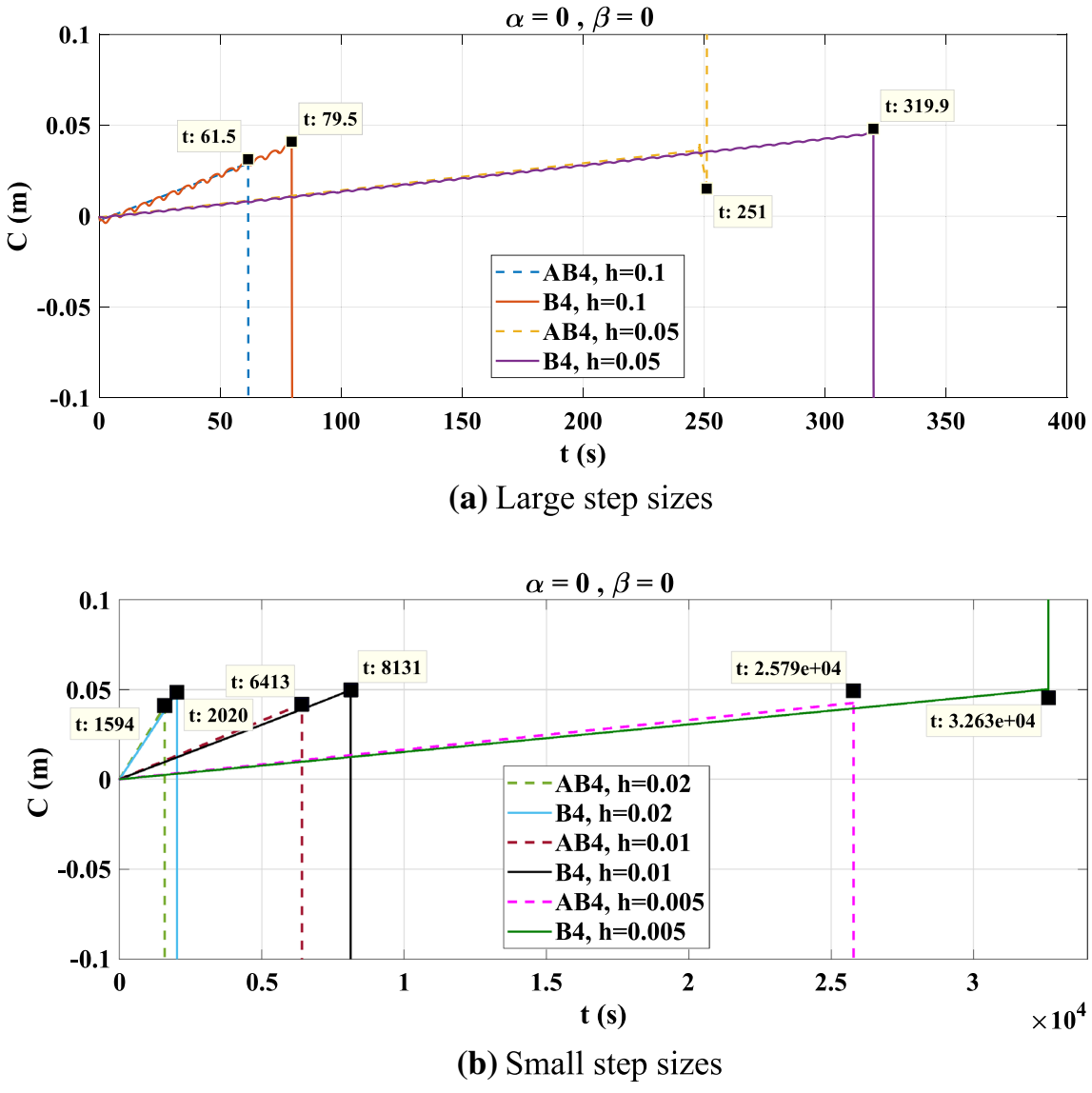

Fig. 5 Error of the 1st constraint equation without stabilization (comparison of collapse points of 4th order of both Adams–Bashforth (AB4) and Bézier (B4) methods using small and large step sizes)

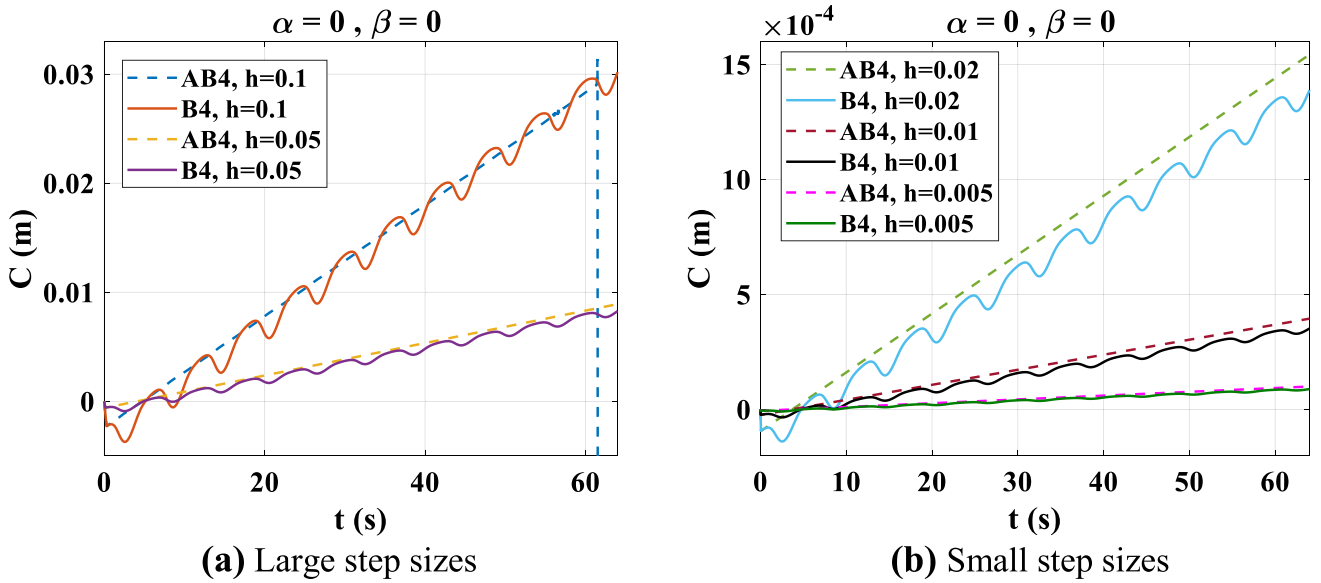

Fig. 6 Error of the 1st constraint equation without stabilization (comparison of 4th order of both Adams–Bashforth (AB4) and Bézier (B4) methods using small and large step sizes)

which would be of interest in the cases where computational cost plays a significant role, such as in real-time problems and complex multibody systems.

5.2.2 Influence of Baumgarte parameters

This subsection presents a study on the influence of Baumgarte parameters in terms of the constraint violations associated with the slider-crank mechanism. Thus, by choosing the Bézier 4th order method as the numerical solution algorithm with assuming the step size of 1 ms and using the Baumgarte stabilization technique, the equations of motion of the mechanism are obtained. With the purpose of checking the stability of the multibody system, the error of the first kinematic constraint and its derivative are examined. Table 4 shows the dominant poles and the results of simulation for different values of Baumgarte parameters. Figures 7 and 8 show the errors for both the first kinematic constraint and its derivative, which confirm the data listed in Table 4.

In case 1 of Table 4, it is expected to observe a divergent response as the parameter $\widehat{\alpha}$ is negative and $|z_p|$ is greater than one. In case 6, although the parameters are positive and therefore, consistent with Baumgarte conditions, the overall result also diverges, because the selected Baumgarte parameters are not within the stability region of the Bézier 4th order method and $|z_p|$ is greater than one. The specific cases 2 and 3 show low convergence speeds, since the size of the dominant pole is close to one in both cases. The angle of the dominant pole is high for case 3 and small for case 2. Therefore, case 3 exhibits oscillations, while case 2 does not exhibit significant oscillations. Finally, cases 4 and 5 present

Table 4 The dominant poles and the results of simulation for different selections of Baumgarte parameters

Case	$\widehat{\alpha}$ and $\widehat{\beta}$	Dominant pole	Result
1	$\widehat{\alpha} = -0.02$ $\widehat{\beta} = +0.00001$	$z = 1.02$ $\|z\| = 1.02, \angle z = 0°$	Diverge
2	$\widehat{\alpha} = 0.1$ $\widehat{\beta} = 0.003$	$z = 0.951 \pm 0.0212i$ $\|z\| = 0.9512, \angle z = 1.278°$	Converge slowly without oscillation
3	$\widehat{\alpha} = 0.03$ $\widehat{\beta} = 0.03$	$z = 0.9699 \pm 0.1706i$ $\|z\| = 0.9848, \angle z = 9.978°$	Converge slowly with oscillation
4	$\widehat{\alpha} = 0.8$ $\widehat{\beta} = 0.2$	$z = 0.6649 \pm 0.1162i$ $\|z\| = 0.6749, \angle z = 9.91°$	Converge fast without oscillation
5	$\widehat{\alpha} = 0.4$ $\widehat{\beta} = 0.5$	$z = 0.4841 \pm 0.4926i$ $\|z\| = 0.6907, \angle z = 45.5°$	Converge fast with oscillation
6	$\widehat{\alpha} = 0.1$ $\widehat{\beta} = 0.55$	$z = 0.5892 \pm 0.8354i$ $\|z\| = 1.022, \angle z = 54.8°$	Diverge

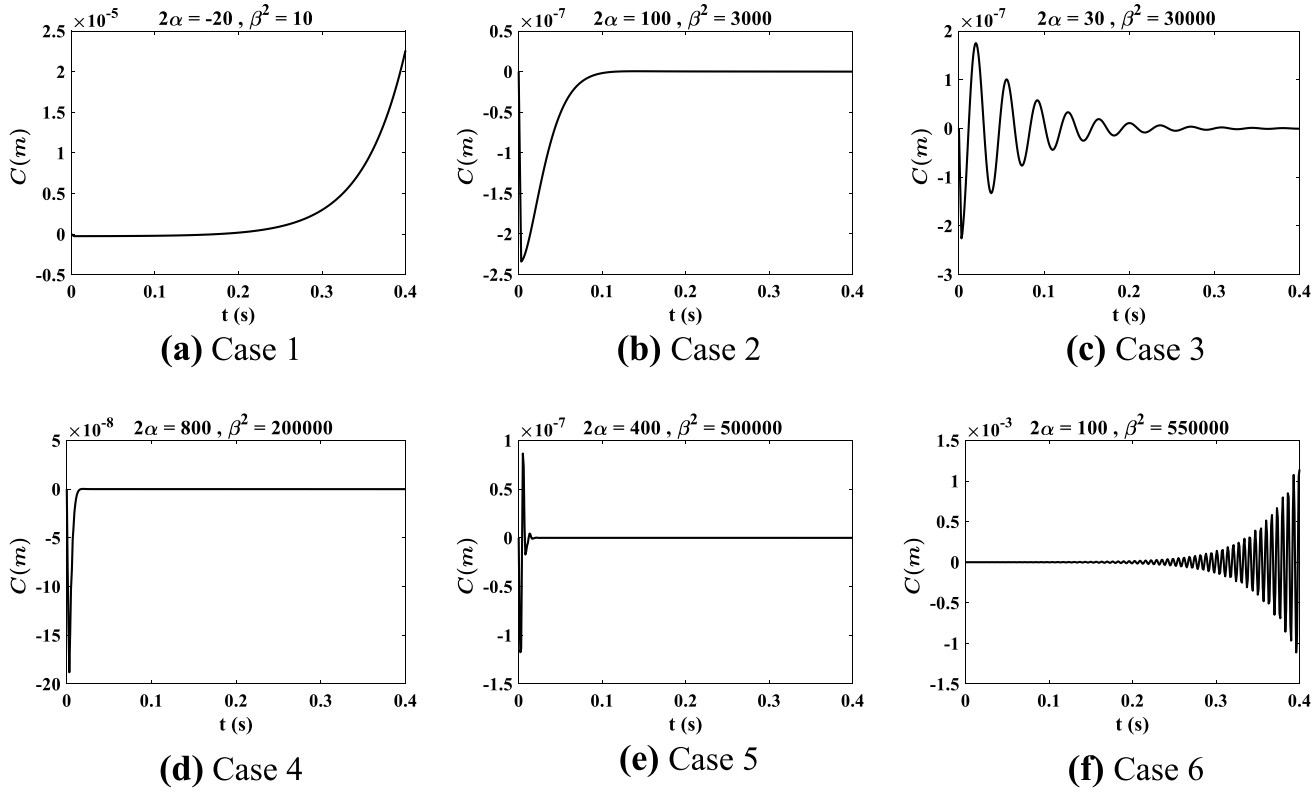

Fig. 7 Error of the 1st constraint equation with different Baumgarte parameters

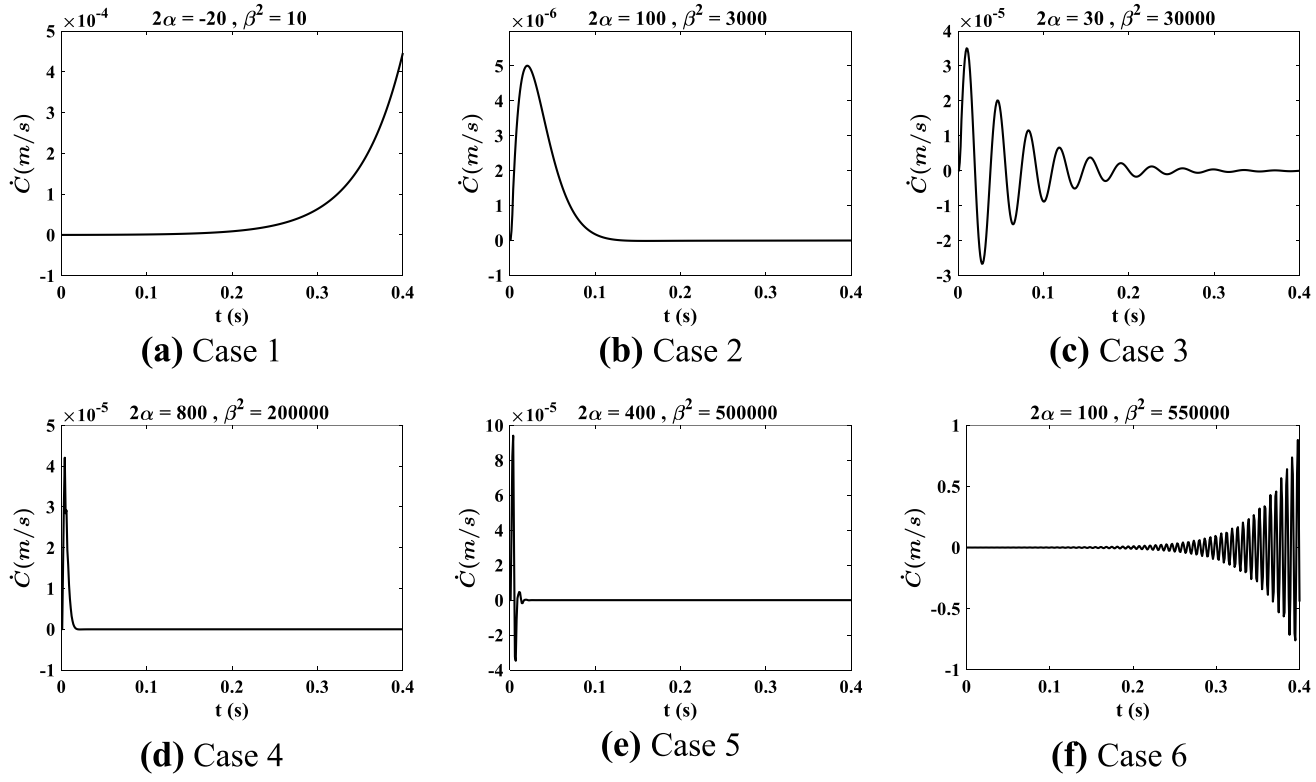

Fig. 8 Error of the derivative of the 1st constraint equation with different Baumgarte parameters

high convergence speeds, since the dominant pole for the Bézier 4th order method is considerably less than one, which clearly suggests the existence of a more stable region. The dominant pole angle is high for case 5 and small for case 4, therefore case 5 shows oscillations, while case 4 exhibits either fewer number of oscillations or no oscillations.

5.2.3 Comparative study for constraint stabilization

In this section, 4th order of the Bézier, Adams–Bashforth and Runge–Kutta methods, are examined. Furthermore, Euler's semi-implicit scheme is compared with the mentioned explicit methods, since it is one of the most simple and popular integration algorithms in real-time simulations. It should be noted that the Bézier and Adams–Bashforth methods are multi-step numerical integration algorithms, while the Runge–Kutta method is a single-step multi-stage numerical integration procedure. The step size for the Bézier, Adams–Bashforth and Euler methods is equal to 1 ms. As mentioned earlier, in order to consider similar computational costs for all methods, the step size of the Runge–Kutta method is 5 times that of the other three methods, that is the time step is equal to 5 ms. With the purpose to compare these methods, the Baumgarte parameters presented in Table 5 have been selected according to the stability regions. The CPU time necessary to solve the equations of motion for each method is reported in Table 6. It can be observed that computational costs are almost the same and the difference between CPU times of each method is less than 4%, which is caused by background apps running on the computer. It must be noticed that the reported CPU times are for 10 s of simulation as it is shown in the plots of Fig. 9 and they represent the average response for 5 simulation trials. The simulations are performed on a laptop with Intel(R) Core(TM) i7-6700HQ CPU @ 2.60GHz, 8.00 GB DDR4 RAM, Windows 10 64-bit and MATLAB 2017.

In the first case presented in Table 5, these parameters are selected in such a way that they are within the stability regions of all methods considered. In the second case, for all methods, they are within the stability regions, but the magnitude of the dominant pole of the Adams–Bashforth method is close to one, and in fact, the parameters for the Adams–Bashforth method are close to the boundary of the stability region. In the third case, with a slight change in the value of $\widehat{\beta}$, the parameters for the Adams–Bashforth method are located outside the region, but close to the boundary of the stability region, and as a result, the size of the dominant pole exceeds one. Moreover, in this particular case, the parameters are within the stability regions of the Bézier, Runge–Kutta and Euler methods. Based on the analysis previously described, it is expected to observe a diverging behavior in the error of constraint and its time derivative for the Adams–Bashforth method, in the third case. Some computational results for these studies are presented in the plots of Fig. 9, from which the following points can be inferred:

1. According to the plots of Fig. 9b, it can be observed that when the Baumgarte parameters are within the stability region and far from the boundaries of the region; the Bézier and Adams–Bashforth methods show almost identical behavior.
2. According to the plots of Fig. 9a, c and f, it is visible that the Runge–Kutta and the Euler's semi-implicit methods have a constant oscillation around the value of zero, and the amplitude of the oscillation is much larger for

Table 6 CPU time consumed for different numerical integration methods

Case	CPU Time (s)			
	Bézier 4th order (step size 1 ms)	Adams–Bashforth 4th order (step size 1 ms)	Runge–Kutta 4th order (step size 5 ms)	Euler semi-implicit (step size 1 ms)
1	8.34	8.41	8.63	8.52
2	8.42	8.38	8.55	8.56
3	8.39	8.42	8.60	8.53

Table 5 Influence of dimensionless Baumgarte parameters on the dominant poles for different numerical integration methods

Case	$\widehat{\alpha}$ and $\widehat{\beta}$	Dominant pole			
		Bézier 4th order	Adams–Bashforth 4th order	Runge–Kutta 4th order	Euler semi-implicit
1	$\widehat{\alpha} = 0.1$	$z = 0.898 \pm 0.299i$	$z = 0.906 \pm 0.291i$	$z = 0.074 \pm 0.740i$	$z = 0.855 \pm 0.281i$
	$\widehat{\beta} = 0.1$	$\lvert z\rvert = 0.947, \angle z = 18.45°$	$\lvert z\rvert = 0.952, \angle z = 17.83°$	$\lvert z\rvert = 0.744, \angle z = 84.27°$	$\lvert z\rvert = 0.9, \angle z = 18.19°$
2	$\widehat{\alpha} = 0.5$	$z = 0.763 \pm 0.142i$	$z = -0.903 \pm 0.428i$	$z = 0.095 \pm 0.237i$	$z = 0.775 \pm 0.097i$
	$\widehat{\beta} = 0.1$	$\lvert z\rvert = 0.776, \angle z = 10.55°$	$\lvert z\rvert = 0.999, \angle z = 154.6°$	$\lvert z\rvert = 0.255, \angle z = 68.15°$	$\lvert z\rvert = 0.781, \angle z = 7.12°$
3	$\widehat{\alpha} = 0.5$	$z = 0.762 \pm 0.144i$	$z = -0.903 \pm 0.433i$	$z = 0.090 \pm 0.241i$	$z = 0.774 \pm 0.098i$
	$\widehat{\beta} = 0.101$	$\lvert z\rvert = 0.776, \angle z = 10.69°$	$\lvert z\rvert = 1.001, \angle z = 154.4°$	$\lvert z\rvert = 0.258, \angle z = 69.45°$	$\lvert z\rvert = 0.780, \angle z = 7.22°$

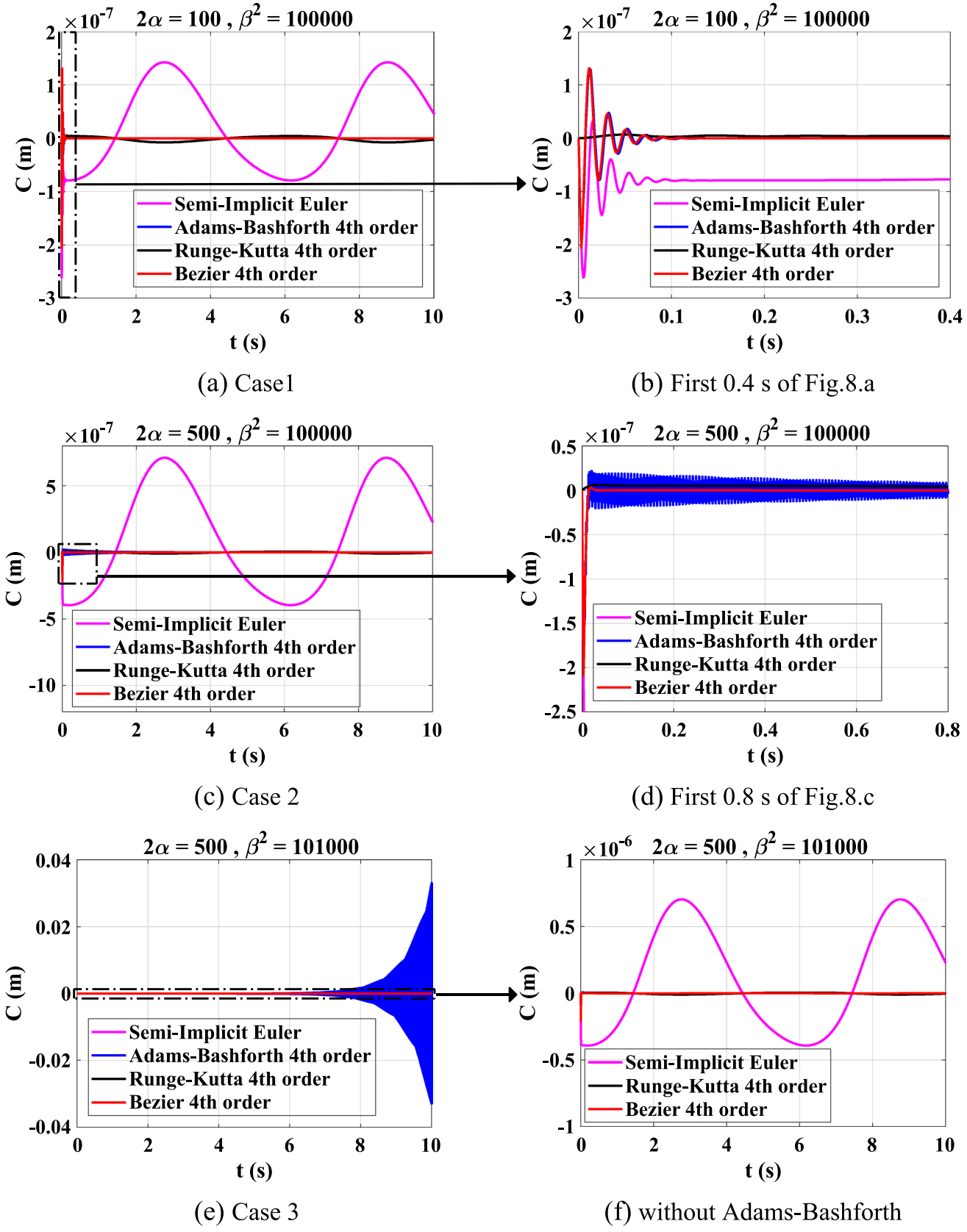

Fig. 9 Influence of the values of $\hat{\alpha}$ and $\hat{\beta}$ on the error of the 1st constraint equation for different numerical methods

the Euler method. For the Bézier and Adams–Bashforth methods, the oscillation is damped out.

3. In the second and third cases plotted in Fig. 9, Baumgarte parameters are close to the boundary of the stability region of the Adams–Bashforth method and the magnitude of $\angle z_p$ is large; therefore, the response of this method exhibits irregular oscillations with very high frequency. In the second case, Fig. 9c and d, the Baumgarte parameters are within the stability region, and therefore, the amplitude of these oscillations gradually decreases and the error of constraint converges to zero. Nevertheless, in the third case, see plots in Fig. 9e, these parameters are outside of the stability region, which results in a gradual increase of the amplitude of the oscillations and therefore divergence of the error of the constraint. These findings confirm the validity and potential of the presented stability analysis.

6 Concluding remarks

In this paper, the criterion for obtaining the appropriate Baumgarte parameters for the Bézier numerical integration method has been investigated. The computational performance of the introduced method is studied by comparing stability regions for different orders of the numerical method with the Adams–Bashforth and Runge–Kutta methods. The primary results revealed that the Bézier method provides a larger stability domain, and therefore, a wider range for selection of Baumgarte parameters compared with the classical alternative approaches. Furthermore, the rate at which the stability region gets smaller by increasing the order of the integration is less for the Bézier method when compared to the Adams–Bashforth method. These findings clearly indicate a better performance of the Bézier method compared to both Adams–Bashforth and Runge–Kutta integration techniques. By analyzing the constraint error resulted from various numerical integration algorithms in the computational simulation for a slider-crank mechanism, two main sets of results were drawn. Firstly, for certain values of Baumgarte parameters, the Adams–Bashforth method became unstable while the Bézier method remained stable. The same observation can be shown for the comparison of the Runge–Kutta and Bézier methods as a result of a larger stability region for the Bézier method. This observation is in line with the predicted behavior based on the presented theory. Secondly, for Runge–Kutta and Euler's semi-implicit methods, a constant oscillation about zero is observed in the plots of constraint error against time, which implies a clear disadvantage of these methods. Considering reasonably high performance of the Bézier based integration scheme, in terms of accuracy and stability, it is expected that the described approach to be considered for different benchmark problems in the context of multibody dynamics.

Appendix

For the slider-crank mechanism mentioned in Sect. 5, the mass matrix can be defined as

$$\mathbf{M} = \mathrm{diag}\left(J_1 \;\; m_2 \;\; m_2 \;\; J_2 \;\; m_3 \right) \tag{20}$$

where J_1 and J_2 represent the mass moment of inertia for bodies 1 and 2, respectively, and m_2 and m_3 indicate masses of bodies 2 and 3. The corresponding constraint Jacobian matrix, vector $\boldsymbol{\gamma}$ and vector $\mathbf{g}$ are expressed as

$$\mathbf{C_q} = \begin{bmatrix} -l_1\sin\theta_1 & -1 & 0 & -\frac{l_2}{2}\sin\theta_2 & 0 \\ l_1\cos\theta_1 & 0 & -1 & \frac{l_2}{2}\cos\theta_2 & 0 \\ 0 & 1 & 0 & -\frac{l_2}{2}\sin\theta_2 & -1 \\ 0 & 0 & 1 & \frac{l_2}{2}\cos\theta_2 & 0 \end{bmatrix} \tag{21}$$

$$\boldsymbol{\gamma} = \begin{bmatrix} l_1\cos\theta_1\dot{\theta}_1^{\,2} + \frac{l_2}{2}\cos\theta_2\dot{\theta}_2^{\,2} \\ l_1\sin\theta_1\dot{\theta}_1^{\,2} + \frac{l_2}{2}\sin\theta_2\dot{\theta}_2^{\,2} \\ \frac{l_2}{2}\cos\theta_2\dot{\theta}_2^{\,2} \\ \frac{l_2}{2}\sin\theta_2\dot{\theta}_2^{\,2} \end{bmatrix} \tag{22}$$

$$\mathbf{g} = \begin{bmatrix} 0 & 0 & m_2 g & 0 & 0 \end{bmatrix}^{\mathrm{T}} \tag{23}$$

Funding No funding was received for conducting this study.

Declarations

Conflict of interest The authors declare that they have no conflict of interest.

References

1. Shabana AA (2010) Computational dynamics, 3rd edn. Wiley, New York
2. Ginsberg JH (2008) Engineering dynamics. Cambridge University Press, New York
3. Lagrange JL (1788) Mécanique analytique, 1st edn. L'Académie Royal des Sciences, Paris
4. Hamilton WR (1834) On a general method in dynamics. Philos Trans R Soc Lond 247–308

5. Gibbs JW (1879) On the fundamental formulae of dynamics. Am J Math 2:49–64. https://doi.org/10.2307/2369196
6. Dirac PAM (1964) Lectures on quantum mechanics. Yeshiva University, New York
7. Kane TR, Wang CF (1965) On the derivation of equations of motion. J Soc Ind Appl Math 13:487–492. https://doi.org/10.1137/0113030
8. Kane TR, Levinson DA (1980) Formulation of equations of motion for complex spacecraft. J Guid Control Dyn 3:99–112. https://doi.org/10.2514/3.55956
9. Udwadia FE, Kalaba RE (1992) A new perspective on constrained motion. Proc R Soc Lond Ser A Math Phys Sci 439:407–410. https://doi.org/10.1098/rspa.1992.0158
10. Talaeizadeh A, Forootan M, Zabihi M, NejatPishkenari H (2020) Comparison of Kane's and Lagrange's methods in analysis of constrained dynamical systems. Robotica. 38:2138–2150. https://doi.org/10.1017/S0263574719001899
11. Marques F, Roupa I, Silva MT, Flores P, Lankarani HM (2021) Examination and comparison of different methods to model closed loop kinematic chains using Lagrangian formulation with cut joint, clearance joint constraint and elastic joint approaches. Mech Mach Theory. https://doi.org/10.1016/j.mechmachtheory.2021.104294
12. Hardell C (1996) An integrated system for computer aided design and analysis of multibody systems. Eng Comput. https://doi.org/10.1007/BF01200259
13. Daberkow A, Kreuzer EJ (1999) Integrated approach for computer aided design in multibody system dynamics. Eng Comput. https://doi.org/10.1007/s003660050011
14. González M, González F, Luaces A, Cuadrado J (2010) A collaborative benchmarking framework for multibody system dynamics. Eng Comput. https://doi.org/10.1007/s00366-009-0139-0
15. Kortelainen J, Mikkola A (2015) Semantic restrictions and rules in applications of multibody dynamics. Eng Comput. https://doi.org/10.1007/s00366-013-0326-x
16. Chen Y, Feng J, Peng X, Sun Y, He Q, Yu C (2021) An approach for dynamic analysis of planar multibody systems with revolute clearance joints. Eng Comput. https://doi.org/10.1007/s00366-020-00935-x
17. Rodrigues da Silva M, Marques F, Tavares da Silva M, Flores P (2022) A comparison of spherical joint models in the dynamic analysis of rigid mechanical systems: ideal, dry, hydrodynamic and bushing approaches. Multibody Syst Dyn. https://doi.org/10.1007/s11044-022-09843-y
18. Celdran A, Saura M, Dopico D (2022) Computational structural analysis of spatial multibody systems based on mobility criteria. Mech Mach Theory. https://doi.org/10.1016/j.mechmachtheory.2022.104985
19. Yuan T, Fan W, Ren H (2023) A general nonlinear order-reduction method based on the referenced nodal coordinate formulation for a flexible multibody system. Mech Mach Theory. https://doi.org/10.1016/j.mechmachtheory.2023.105290
20. Go MS, Han S, Lim JH, Kim JG (2023) An efficient fixed-time increment-based data-driven simulation for general multibody dynamics using deep neural networks. Eng Comput. https://doi.org/10.1007/s00366-023-01793-z
21. Boyce WE, DiPrima RC (2012) Elementary differential equations and boundary value problems, 10th edn. Wiley, Hoboken
22. Marques F, Souto AP, Flores P (2017) On the constraints violation in forward dynamics of multibody systems. Multibody Syst Dyn 39:385–419. https://doi.org/10.1007/s11044-016-9530-y
23. Baumgarte J (1972) Stabilization of constraints and integrals of motion in dynamical systems. Comput Methods Appl Mech Eng 1:1–16. https://doi.org/10.1016/0045-7825(72)90018-7
24. Wehage RA, Haug EJ (1982) Generalized coordinate partitioning for dimension reduction in analysis of constrained dynamic systems. J Mech Des Trans ASME 104:247–255. https://doi.org/10.1115/1.3256318
25. Bayo E, Garcia De Jalon J, Serna MA (1988) A modified lagrangian formulation for the dynamic analysis of constrained mechanical systems. Comput Methods Appl Mech Eng 71:183–195. https://doi.org/10.1016/0045-7825(88)90085-0
26. Chang CO, Nikravesh PE (1985) An adaptive constraint violation stabilization method for dynamic analysis of mechanical systems. J Mech Des Trans ASME 107:488–492. https://doi.org/10.1115/1.3260750
27. Yoon S, Howe RM, Greenwood DT (1995) Stability and accuracy analysis of baumgarte's constraint violation stabilization method. J Mech Des Trans ASME 117:446–453. https://doi.org/10.1115/1.2826699
28. Ostermeyer GP (1990) On Baumgarte stabilization for differential algebraic equations. Real-Time Integr Methods Mech Syst Simul. https://doi.org/10.1007/978-3-642-76159-1_10
29. Lin ST, Hong MC (1998) Stabilization method for numerical integration of multibody mechanical systems. J Mech Des Trans ASME 120:565–572. https://doi.org/10.1115/1.2829316
30. Lin ST, Huang JN (2002) Stabilization of Baumgarte's method using the Runge–Kutta approach. J Mech Des Trans ASME 124:633–641. https://doi.org/10.1115/1.1519277
31. Flores P, MacHado M, Seabra E, Tavares Da Silva M (2011) A parametric study on the baumgarte stabilization method for forward dynamics of constrained multibody systems. J Comput Nonlinear Dyn 6:1–9. https://doi.org/10.1115/1.4002338
32. Kim JK, Chung IS, Lee BH (1990) Determination of the feedback coefficients for the constraint violation stabilization method. Proc Inst Mech Eng Part C J Mech Eng Sci 204:233–242. https://doi.org/10.1243/PIME_PROC_1990_204_101_02
33. Ascher UM, Chin H, Reich S (1994) Stabilization of DAEs and invariant manifolds. Numer Math 67:131–149. https://doi.org/10.1007/s002110050020
34. Ascher UM, Chin H, Petzold LR, Reich S (1995) Stabilization of constrained mechanical systems with DAEs and invariant manifolds. Mech Struct Mach 23:135–157. https://doi.org/10.1080/08905459508905232
35. Guizhi L, Rong L (2018) Determination of stability correction parameters for dynamic equations of constrained multibody systems. Math Probl Eng. https://doi.org/10.1155/2018/8945301
36. Park KC, Chiou JC (1988) Stabilization of computational procedures for constrained dynamical systems. J Guid Control Dyn 11:365–370. https://doi.org/10.2514/3.20320
37. Park KC, Chiou JC, Downe JD (1990) Explicit-implicit staggered procedure for multibody dynamics analysis. J Guid Control Dyn 13:562–570. https://doi.org/10.2514/3.25370
38. Bayo E, Avello A (1994) Singularity-free augmented Lagrangian algorithms for constrained multibody dynamics. Nonlinear Dyn 5:209–231. https://doi.org/10.1007/BF00045677
39. Weijia Z, Zhenkuan P, Yibing W (2000) An automatic constraint violation stabilization method for differential/ algebraic equations of motion in multibody system dynamics. Appl Math Mech 21:103–108. https://doi.org/10.1007/BF02458546
40. Blajer W (2002) Augmented Lagrangian formulation: geometrical interpretation and application to systems with singularities and redundancy. Multibody Syst Dyn 8:141–159. https://doi.org/10.1023/A:1019581227898
41. Hong M, Choi MH, Jung S, Welch S, Trapp J (2005) Effective constrained dynamic simulation using implicit constraint enforcement. Proc IEEE Int Conf Robot Autom. https://doi.org/10.1109/ROBOT.2005.1570816

42. Hong M, Welch S, Trapp J, Choi MH (2006) Implicit constraint enforcement for rigid body dynamic simulation. Lect Notes Comput Sci. https://doi.org/10.1007/11758501_67
43. Braun DJ, Goldfarb M (2009) Eliminating constraint drift in the numerical simulation of constrained dynamical systems. Comput Methods Appl Mech Eng 198:3151–3160. https://doi.org/10.1016/j.cma.2009.05.013
44. Nada A, Bayoumi M (2023) Development of a constraint stabilization method of multibody systems based on fuzzy logic control. Multibody Syst Dyn. https://doi.org/10.1007/s11044-023-09921-9
45. Laulusa A, Bauchau OA (2008) Review of Classical Approaches for Constraint Enforcement in Multibody Systems. J Comput Nonlinear Dyn. https://doi.org/10.1115/1.2803257
46. Bauchau OA, Laulusa A (2008) Review of contemporary approaches for constraint enforcement in multibody systems. J Comput Nonlinear Dyn. https://doi.org/10.1115/1.2803258
47. Aghdam MM, Haghi P, Fallah A (2015) Nonlinear initial value ordinary differential equations. Nonlinear Approaches Eng Appl. https://doi.org/10.1007/978-3-319-09462-5_5
48. Heydarpour Y, Aghdam MM (2016) A hybrid Bézier based multi-step method and differential quadrature for 3D transient response of variable stiffness composite plates. Compos Struct 154:344–359. https://doi.org/10.1016/j.compstruct.2016.07.060
49. Heydarpour Y, Aghdam MM (2016) A novel hybrid Bézier based multi-step and differential quadrature method for analysis of rotating FG conical shells under thermal shock. Compos Part B Eng 97:120–140. https://doi.org/10.1016/j.compositesb.2016.04.055
50. Kabir H, Aghdam MM (2019) A robust Bézier based solution for nonlinear vibration and post-buckling of random checkerboard graphene nano-platelets reinforced composite beams. Compos Struct 212:184–198. https://doi.org/10.1016/j.compstruct.2019.01.041
51. Kabir H, Aghdam MM (2021) A generalized 2D Bézier-based solution for stress analysis of notched epoxy resin plates reinforced with graphene nanoplatelets. Thin-Walled Struct. 169:108484. https://doi.org/10.1016/j.tws.2021.108484
52. Gerald CF, Wheatley PO (1999) Applied numerical analysis. Addison-Wesley, Reading
53. Farin G (2002) Curves and surfaces for CAGD. A practical guide, 5th edn. Elsevier Ltd, San Francisco, p 2002
54. Roupa I, Gonçalves SB, da Silva MT (2023) Kinematics and dynamics of planar multibody systems with fully Cartesian coordinates and a generic rigid body. Mech Mach Theory. https://doi.org/10.1016/j.mechmachtheory.2022.105134
55. Ruggiu M, González F (2023) A benchmark problem with singularities for multibody system dynamics formulations with constraints. Multibody Syst Dyn 58:181–196. https://doi.org/10.1007/s11044-023-09896-7
56. García de Jalón J, Gutiérrez-López MD (2013) Multibody dynamics with redundant constraints and singular mass matrix: Existence, uniqueness, and determination of solutions for accelerations and constraint forces. Multibody Syst Dyn. https://doi.org/10.1007/s11044-013-9358-7
57. Ogata K (1995) Discrete-time control systems, 2nd edn. Prentice-Hall, Prentice
58. Polyanin AD, Zaitsev VF (2003) Handbook of exact solutions for ordinary differential equations, 2nd edn. Chapman and Hall/CRC Press, Boca Raton
59. Franklin GF, Powell JD, Emami-Naeini A (1994) Feedback control of dynamic systems, 3rd edn. Addison-Wesley, Reading
60. Nikravesh PE (2007) Initial condition correction in multibody dynamics. Multibody Syst Dyn. https://doi.org/10.1007/s11044-007-9069-z